Altered neural oscillations within and between sensorimotor cortex and parietal cortex in chronic jaw pain

Wei-en Wang[a], Arnab Roy[a], Gaurav Misra[b], Rachel L.M. Ho[a], Margarete C. Ribeiro-Dasilva[c], Roger B. Fillingim[d], Stephen A. Coombes[a],*

[a] Laboratory for Rehabilitation Neuroscience, Department of Applied Physiology and Kinesiology, University of Florida, Gainesville, FL, United States of America
[b] Short Proof LLC, CA, United States of America
[c] Department of Restorative Dental Science, University of Florida, Gainesville, FL, United States of America
[d] Department of Community Dentistry and Behavioral Science, University of Florida, Gainesville, FL, United States of America

A B S T R A C T

Pain perception is associated with priming of the motor system and the orienting of attention in healthy adults. These processes correspond with decreases in alpha and beta power in the sensorimotor and parietal cortices. The goal of the present study was to determine whether these findings extend to individuals with chronic pain. Individuals with chronic jaw pain and pain-free controls anticipated and experienced a low pain or a moderate pain-eliciting heat stimulus. Although stimuli were calibrated for each subject, stimulus temperature was not different between groups. High-density EEG data were collected during the anticipation and heat stimulation periods and were analyzed using independent component analyses, EEG source localization, and measure projection analyses. Direct directed transfer function was also estimated to identify frequency specific effective connectivity between regions. Between group differences were most evident during the heat stimulation period. We report three novel findings. First, the chronic jaw pain group had a relative increase in alpha and beta power and a relative decrease in theta and gamma power in sensorimotor cortex. Second, the chronic jaw pain group had a relative increase in power in the alpha and beta bands in parietal cortex. Third, the chronic jaw pain group had less connectivity strength in the beta and gamma bands between sensorimotor cortex and parietal cortex. Our findings show that the effect of chronic pain attenuates rather than magnifies neural responses to heat stimuli. We interpret these findings in the context of system-level changes in intrinsic sensorimotor and attentional circuits in chronic pain.

1. Introduction

Over the last several decades, fundamental advances have been made in our understanding of how the brain processes acute pain in healthy adults (Apkarian et al., 2005; Coghill et al., 1999; Schulz et al., 2015; Tracey and Mantyh, 2007; Wager et al., 2013). Task-based experiments using electroencephalography (EEG) and magnoencephalography (MEG) generally show that acute pain is associated with decreases in alpha and beta power in the sensorimotor cortex and the parietal cortex, and increases in theta and gamma power in the medial and ventral prefrontal cortex, and anterior cingulate cortex (Gross et al., 2007; Misra et al., 2017b; Schulz et al., 2015; Schulz et al., 2011; Zhang et al., 2012). In healthy adults, these neural oscillations have been interpreted as reflecting disinhibition in sensorimotor and attentional circuits, as individuals orient their attention to the pain-eliciting stimulus and prime their motor system for action (Foxe and Snyder, 2011; Misra et al., 2016; Peng et al., 2015). The goal in the current study was to determine whether chronic pain enhances or attenuates neural oscillations to an acute pain-eliciting stimulus.

In chronic pain, changes within and between sensorimotor and attentional networks have been evidenced during resting states (Case et al., 2017; de Tommaso et al., 2015; de Vries et al., 2013; González-Roldán et al., 2016; Sarnthein et al., 2006; Stern et al., 2006; Vanneste et al., 2017), with increases, rather than decreases in beta power more often associated with chronic pain. Indeed, increased beta power in regions including the primary and secondary sensorimotor cortices, dorsal-lateral prefrontal cortex, midcingulate cortex, rACC, and insula have been reported across cohorts of patients with fibromyalgia (González-Roldán et al., 2016; Lim et al., 2016; Vanneste et al., 2017), chronic neuropathic pain (Sarnthein et al., 2006; Stern et al., 2006), and sickle cell disease (Case et al., 2017). In contrast to the task-based approach that is necessary to study pain in healthy adults, there is very little evidence of how chronic pain modulates neural oscillations during an acute pain-eliciting stimulus.

We have previously shown that pain-eliciting heat stimuli applied to the upper limb evokes decreases in alpha and beta power in the contralateral sensorimotor cortex (Misra et al., 2017b, 2016). Here, we leverage this task-based paradigm to understand neural oscillations in a

* Corresponding author at: University of Florida, Laboratory for Rehabilitation Neuroscience, Department of Applied Physiology and Kinesiology, PO Box 118206, United States of America.
E-mail address: scoombes@ufl.edu (S.A. Coombes).

cohort of individuals with chronic jaw pain. Thermal stimuli were delivered to the forearm for 5 s while we recorded high-density EEG. The rationale for stimulating the subject's forearm rather than jaw, was to avoid potential between group differences that are focal to the jaw area in orofacial pain including lower pain thresholds in the masseter and anterior temporalis muscles (Farella et al., 2000; Hansdottir and Bakke, 2004), elevated levels of IL-6, IL-7, IL-8 and IL-13 in the masseter muscle (Louca Jounger et al., 2017), and elevated levels of elastin-derived peptides and IL-6 in the synovial fluid (Kaneyama et al., 2002; Kobayashi et al., 2017). EEG data were analyzed using time-frequency analysis, source-localization analysis, and measure projection analysis (MPA) (Bigdely-Shamlo et al., 2013), which together allowed us to characterize neuronal activity at different frequency bands in source space. Given previous *f*MRI studies that show changes in resting state functional connectivity between cortical regions in chronic pain (Kucyi and Davis, 2015; Kutch et al., 2017), we also examined whether chronic pain alters effective connectivity during the heat stimulus. We test the hypothesis that compared to the control group, individuals with chronic jaw pain will show less reduction in alpha and beta power in sensorimotor regions during the pain-eliciting stimulus. In addition, we hypothesize that effective connectivity between cortical regions will be different between groups.

2. Materials and methods

2.1. Participants

Eighteen human participants with chronic jaw pain, and sixteen pain-free age-matched controls were recruited in the study. Table 1 lists specific details for each group. The recruitment of the jaw pain participants was based on the temporomandibular disorder pain-screening questionnaire. All cases met the following criteria: (1) pain is always present in jaw and temporal area on either side for the last 30 days; (2) have pain or stiffness in jaw on awakening in the last 30 days; and (3) participants reported at least three of the following activities changed pain in their jaw or temporal area in the last 30 days: (a) chewing hard or tough food; (b) opening the month or moving the jaw forward or to

the side; (c) jaw habits such as holding teeth together, clenching, grinding or chewing gum; (d) other activities such as talking, kissing or yawning. Controls were recruited from the local community through flyers. Exclusion criteria for healthy controls included any self-reported history of neurological disease, psychiatric conditions, and any history of chronic pain or current acute pain. Participants were asked to refrain from consuming caffeine and using any hair products on the day of testing. Before experimental testing, participants provided informed consent. This experimental study was approved by the University of Florida Institutional Review Board.
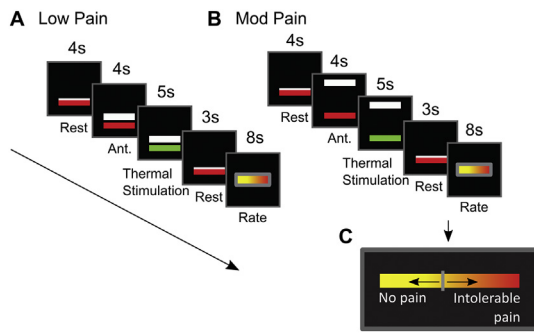
2.2. Clinical evaluation

The chronic jaw pain group and control group were comparable in age [$t(32) = -0.39, p > .05$] and sex $X^2(1, N = 34) = 0.37, p > .05$). Thirteen females and five males were included in the jaw pain group; ten females and six males were included in the control group. Table 1 lists the mean and standard deviations of age and sex for each group. All of the participants in the jaw pain group had jaw pain for a period of at least 3 months. To characterize the chronic jaw pain group, independent *t*-tests were performed on the self-report measurements, including the jaw functional limitation scale (JFLS) (Ohrbach et al., 2008), the Graded Chronic Pain Scale (GCPS) (Von Korff et al., 1992), Oral Behavior Checklist (OBC) (Markiewicz et al., 2006) and Patient-Reported Outcomes Measurement Information System (PROMIS) questionnaires, including fatigue, anxiety and depression (Promis et al., 2007). Significance level was set at $p < .05$.

2.3. Thermal stimulation

Thermal stimuli were delivered to the right forearm of the participants using a 573-mm^2 contact heat-evoked potential stimulator thermode (Pathway System; Medoc Advanced Medical Systems, Durham, NC). The thermode was set to heat up at a rate of 70 °C/s and cool down at a rate of 40 °C/s. From baseline, pain-eliciting temperatures (~45 °C) were therefore reached in ~0.2 s. The onset and offset of heat were precisely controlled. Before the experiment, we used a calibration paradigm to determine the temperatures to elicit low pain and moderate pain for each participant. The two different levels of stimulus intensity were used to determine whether potential between group differences in cortical processing are independent of stimulus intensity. We identified a temperature just above each subject's pain threshold to be the low pain temperature and the temperature corresponding to a rating of 3–4 VAS (out of 10) was used for the moderate pain condition. During the calibration, participants sequentially experienced 18 peusorandomized temperatures that ranged from 40 °C to 48 °C. Each trial lasted for 5 s, and the trials were separated by 17 s of rest. After each stimulation, participants used a scroll wheel to rate the pain on a visual analog scale (VAS) presented on a screen in front of them. The scale ranged from 0 to 10, with 0 being "no pain" and 10 being "intolerable pain". No numbers were visible to the participant. Intolerable pain was defined as the temperature at which the thermode had to be removed from the forearm. After calibration, each participant then completed a training session to become familiar with the paradigm.

2.4. Experimental design and task

We collected high-density EEG data while participants experienced low-pain or moderate-pain eliciting stimuli. Participants completed 96 trials in total. Trials were split into four blocks of 24 trials. Each block consisted of 12 low pain trials and 12 moderate pain trials. Each participant therefore completed a total of 48 low pain trials and 48 moderate pain trials. The delivery of a low pain trial and a moderate pain trial were randomized within a block and the same condition never occurred > 4 times in a row. After each experimental block (24 trials), participants had a 3-min break. Block order was counterbalanced across

Table 1
Group demographics, chronic pain measures and psychological measures for the chronic jaw pain group and the pain-free healthy controls.

	Control ($n = 16$)		Jaw pain group ($n = 18$)		*P*-value
	M	SD	M	SD	
Age	31.31	10.85	32.78	10.84	> 0.05
Gender (Male/Female)	6/10		5/13		> 0.05
Duration of pain (months)	0	0	84.83	71.94	< 0.05
JFLS-20					
Mastication (0–60)	0.25	1.00	15.06	8.23	< 0.05
Jaw mobility (0–40)	0.00	0.00	9.56	5.90	< 0.05
Emotional and verbal expression (0–80)	0.00	0.00	6.44	7.23	< 0.05
GCPS					
Disability days (last 6 months)	0.00	0.00	109.61	66.64	< 0.05
Characteristic pain intensity (0–100)	0.00	0.00	44.63	17.42	< 0.05
Disability score (0–100)	0.00	0.00	17.41	18.81	< 0.05
OBC (0–100)	12.06	9.69	27.56	8.79	< 0.05
PROMIS					
Fatigue 8a (0–40)	7.00	7.26	13.00	8.60	< 0.05
Anxiety 8a (0–40)	6.56	6.94	9.89	5.46	> 0.05
Depression 8a (0–40)	2.88	3.96	4.83	3.90	> 0.05

M = Mean. SD = Standard deviation. JFLS-20 = Jaw Functional Limitation Scale 20-item. GCPS = Graded Chronic Pain Scale. OBC = Oral Behavioral Checklist. PROMIS = Patient-Reported Outcomes Measurement Information System.

Fig. 1. Setup and trial timeline. The experiment was comprised of two conditions: low pain and moderate pain-eliciting stimuli, delivered to the right forearm. A. Participant's view of the screen during a low pain trial. The trial started with a 4-s rest period and was followed by a 4-s anticipation period (Ant.). During the anticipation period, the white bar was separated from the baseline red bar. Thereafter, the thermode was heated to a participant-specific and condition-specific temperature and stayed on for 5-s. As the white bar returned to the baseline position, the temperature of the thermode dropped to baseline and a 3-s period of rest began. A rating bar then appeared on the screen for 8-s and participant gave ratings using the VAS shown in Figure C. B. The participant's view of the screen during a pain trial. Stimulus intensity and the relative position of the white bar were the only differences between trials. Each block of trials included 24 trials – 12 low pain trials and 12 moderate pain trials, which were delivered in a pseudorandomized order. A total of four blocks were performed. C. The visual analog scale (VAS) for pain rating. Extreme left indicates no pain whereas extreme right indicates intolerable pain. Mod = moderate.

participants. Participants sat in a chair with the right arm supinated. Fig. 1 shows the timeline of events during a low pain trial and a moderate pain trial. The trial started with a 4-s rest period. During the rest period, the red bar was stacked on top of the white bar. Then it was followed by a 4-s anticipation period (Ant.) during which the white bar was separated from the red bar. During the anticipation period, participants were informed about the condition of the upcoming trial (i.e. low pain or moderate pain) by seeing the location of the white bar. When the red force bar changed color to green, either low pain or moderate pain was delivered for 5 s. As the white bar returned to the baseline position, the temperature of the thermode returned to baseline and a 3 s rest period began. Participants then rated the pain they experienced using the visual analog scale (VAS) shown in Fig. 1C. The rating curser began in the middle of the VAS scale for each trial. The VAS was visible for 8 s. Participants used a scroll wheel held in their supinated right hand to record their pain rating for that trial.

2.5. Data acquisition

The MotionMonitor system (Innovative Sports Training, Chicago, IL) was configured to record data in real time from the EEG system. A custom LabVIEW program was used to control the visual display and trigger the thermode in synchrony with the EEG recordings.

2.6. EEG data acquisition

EEG data were collected with the ActiveTwo system that comprised 128 Ag-AgCl active electrodes and a 256-channel AD-box (BioSemi, Amsterdam, Netherlands). The ActiveTwo system replaces the conventional ground electrode with two separate electrodes: common mode sense and driven right leg. These two electrodes form a feedback loop, which drives the average potential of the participant as close as possible to the reference voltage in the AD-box. The electrode offsets (the running averages of the voltages measured between the common mode sense and each active electrode) were measured before the start of each session and were kept below 40 μV. EEG signals were sampled

at 2048 Hz for recording the raw data. Data were downsampled to 1000 Hz for analysis. The electrode offset served as an indirect measure of impedance tolerance. Electrode offset was monitored throughout the recording session to ensure that a stable and moderate quality signal was recorded from each active electrode.

2.7. EEG data preprocessing

EEG data were analyzed using the EEGLAB Toolbox (Delorme and Makeig, 2004) for MATLAB (version 2014a; MathWorks, Natick, MA) and custom MATLAB scripts. Fig. 2 provides an overview of the steps of the EEG analysis. The original continuous data were high-pass filtered at 1 Hz and low-pass filtered at 90 Hz. A notch filter of 55–65 Hz using a Kaiser window was also applied. All the filters were zero-phase FIR filters. In order to remove artifacts in the EEG signals, two stages of data preprocessing and trial rejection were conducted: (1) Within-trial assessment (Fig. 2A): EEG channels were screened and detected as artifacts as follows. For a given trial, a channel was marked if > 2% of its data points were greater than four standard deviations from the mean channel data. Furthermore, if a trial contained more than seven marked channels (5% of all channels), the trial was excluded from the analysis. If a trial contained less than seven marked channels, marked channels were interpolated using neighboring channels. EEG signals were then re-referenced to the global average of all EEG channels and the CleanLine function was applied (Bigdely-Shamlo et al., 2015). The onset of anticipation was defined as the event for aligning the EEG signal across trials. Thereafter, 10-s epochs, from 2 s before the event to 8 s after the event (4-s anticipation, 4-s heat stimulation) were extracted from each trial and aligned at anticipation onset. (2) Across-trial assessment (Fig. 2B): after concatenating all the epoched data for each participant, data were downsampled to 250 Hz. Trials with extreme values (> 75 μV in any channel) (Wang et al., 2016), an improbable occurrence of data distribution across epochs (> 4 SDs of the single- and all-channel mean probability distribution), or an abnormal distribution (> 4 SDs of the single- and all-channel mean kurtosis value) were excluded from further analyses (Delorme and Makeig, 2004).

2.8. Independent component analysis and artifact removal

EEG data were prepared for further analysis by concatenating all epochs across all conditions within each participant. The infomax independent component analysis (ICA) algorithm (Platt and Haykin, 1995) with the natural gradient feature (Amari, 1998) was used to decompose the concatenated EEG data of each participant into maximally independent components (Fig. 2C). The ICA enabled automated detection and removal of stereotyped eye, muscle, and line noise artifacts. We used the Multiple Artifact Rejection Algorithm (MARA) Toolbox for automated artifact rejection (Winkler et al., 2014) with custom modifications to optimize the algorithm for our data (Fig. 2D). MARA uses a linear, pretrained classifier that performs a binary classification (artifact or nonartifact) in a 6D feature space. The prior probability value was set to 0.1 to ensure that the MARA Toolbox did not reject nonartifactual components in our dataset. After artifact rejection based on MARA, visual inspection of each IC was conducted and ICs were removed based on each IC's spectrum, scalp topography, and dipole fit. A second round of ICA was then run to maximize brain source-related independent components (Fig. 2E).

2.9. EEG source localization

Source localization of each independent component was performed using the DIPFIT Toolbox (Delorme et al., 2011), which computes an equivalent current dipole model that best explains the scalp topography of each independent component (Fig. 2F). An equivalent current dipole model was fitted using a nonlinear optimization technique (Scherg, 1990) and the analytical spherical head model from Brain Electrical
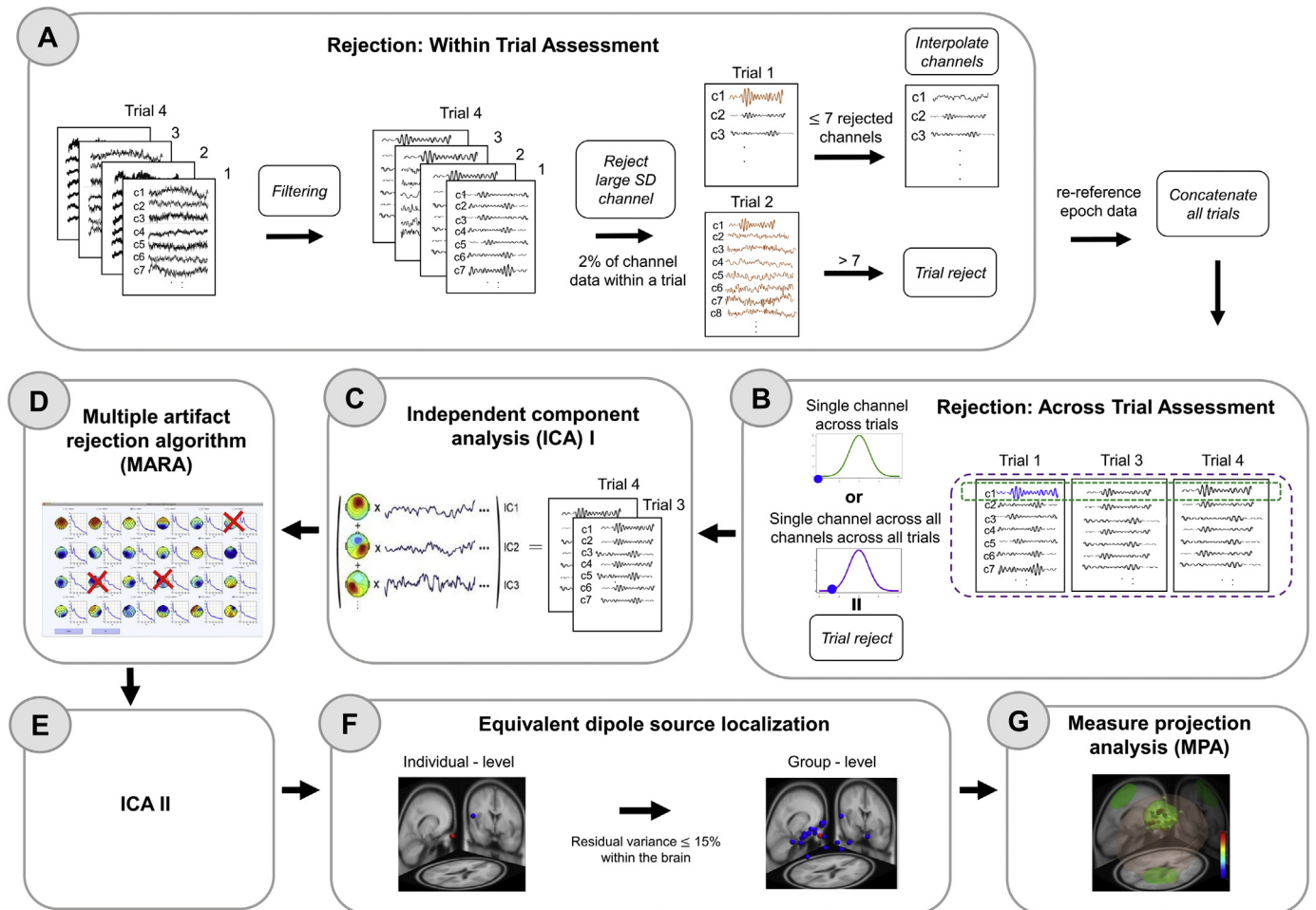
Fig. 2. Overview of the EEG analysis. A. Applying filter and within-trial assessment. B. Across-trial assessment. C. Independent component analysis (ICA). D. Automated artifact rejection using the Multiple Artifact Rejection Algorithm (MARA) Toolbox. E. Second implementation of ICA. F. Source localization of each independent component using the DIPFIT Toolbox. G. Comparison and inferences of multi-subject EEG independent components using the measure projection toolbox (MPA).

Source Analysis (BESA; Gräfelfing, Germany), which uses four spherical surfaces (skin, skull, cerebrospinal fluid, and cortex) to model the electrical properties of the human head (Kavanagk et al., 1978). The actual channel location map was mapped onto the BESA template channel location map, which in turn, was coregistered to the Montreal Neurological Institute (MNI) brain template. Dipoles were excluded if they were located outside of the MNI brain, or if their residual variance was > 15% (Misra et al., 2017b; Roy et al., 2018a).

2.10. EEG measure projection analysis

Measure projection analysis (MPA) is a statistical method for characterizing the localization and consistency of EEG measures across participants of EEG (Bigdely-Shamlo et al., 2013) (Fig. 2G). It allows the use of EEG as a 3D cortical imaging modality with near-centimeter-scale spatial resolution. We have previously used this approach to analyze high density EEG data (Misra and Coombes, 2015; Ofori et al., 2015). MPA was used through the Measure Projection Toolbox of EEGLAB and included the following five steps: (1) the locations of dipoles were overlaid on a 3D grid of voxels placed with 8 mm spacing inside the MNI brain template (27*23*23 voxels). (2) EEG measures for the dipole-localized independent components were spatially smoothed using a truncated 3D spatial Gaussian kernel. The SD of the Gaussian was set to 12 mm, and its extent was truncated to three SD (36 mm) to prevent spurious effects from distant dipoles. (3) A pairwise independent component similarity matrix was constructed by calculating

the signed mutual information between each independent component pair measure. The similarity matrix was used to calculate convergence, which was the voxel-wise, expected value of measure similarity. Convergence was a scalar and was larger for areas in which the measures associated with local independent components were similar. A *p*-value for the convergence value at each voxel was set at 0.01. (4) Within the measure convergence subspace, distinguishable spatial domains were formed by thresholding-based affinity propagation clustering based on a similarity matrix across all the dipoles from all subjects. Similarity matrices of pairwise correlations between projected measures at each voxel position were grouped into clusters, referred to as domains, based on the maximum allowed correlation between cluster exemplars. Maximal exemplar-pair similarity was set to a correlation value of 0.8, which is similar to previous studies (Misra et al., 2017b; Ofori et al., 2015). To define anatomical regions, the toolbox incorporates the probabilistic atlas of human cortical structures provided by the Laboratory of Neuro Imaging (LONI) project (Shattuck et al., 2008). (5) Group difference testing was implemented, where for each identified domain, statistical significance of differences between the control group and the chronic jaw pain group on the event-related spectral perturbation (ERSP) measures at a given condition (i.e. low pain and moderate pain condition) was computed. First, it projected the measure associated with each group at each condition to each voxel in the domain, producing the projected measure. Then the projected measure at a voxel was weighted by the dipole density at that voxel, summed across all domain voxels, and normalized by the total domain voxel

density to obtain a weighted-mean measure across all domain voxels.

2.11. EEG measures

ERSP was calculated for each independent component that was source localized within the MNI brain template (Makeig et al., 2004). Sinusoidal wavelet transforms were used to convert the independent component EEG data from the time domain to the time-frequency domain to obtain the spectral estimate at each frequency and time point for each trial. The 2-s time window before the anticipation period served as the baseline relative to which spectral perturbations were calculated over the subsequent 8 window. The 8-s window included the 4-s anticipation period and the 4-s heat stimulation period. Spectral estimates after the onset of anticipation were baseline normalized by subtracting the mean baseline log-power spectrum from each spectral estimate. The complex norms of the normalized spectral estimates were squared and averaged across trials to obtain the ERSP value at each frequency (3–90 Hz) across the entire 10-s time window. The range of frequencies within each band and their corresponding labels were based on previous literature and follow established convention (theta, 3–8 Hz; alpha, 8–13 Hz; beta, 13–30 Hz; gamma, 70–90 Hz) (Berger, 1929; Hari et al., 2018; Misra et al., 2017a; Noachtar et al., 1999; Schulz et al., 2015).

2.12. Estimating participant-specific ERSP at each domain

The ERSP matrix of each IC was 200 cells along the time domain (1.26 s before and 7.26 s after the heat onset, truncated by the sinusoidal wavelet transformation), and 100 cells along the frequency domain (3 Hz – 90 Hz) on a logarithmic scale. For a given domain, for each participant per condition, a mean ERSP matrix was developed by first choosing all participant-specific dipoles that contributed to the domain and then averaging across the dipoles. Permutation t-test with 1000 samples were applied to the subject-mean projected ERSP measures to determine significant differences between groups for each condition as done in our previous work (Chung et al., 2017; Misra et al., 2017b). Between group contrast plots (time x frequency) were therefore generated for the low pain and moderate pain conditions for each domain. All p-values from all contrast plots for all domains were then concatenated and simultaneously corrected using the FDR correction to stringently control for multiple comparisons (Benjamini and Hochberg, 1995). That is, following the permutation tests, p-values from each matrix (100 × 200 elements = 20,000 elements per contrast) for each contrast plot (2 per domain) for all domains (5 domains) were concatenated and simultaneously corrected using the FDR correction. P-values were therefore corrected across 200,000 elements.

2.13. Correlations between ERSP and pain intensity and stimulus intensity

To investigate the relationship between the ERSP and the pain measures [i.e. pain intensity ratings and stimulus intensity], a pixel-based partial Spearman Rho correlation test was conducted in each domain across the two conditions for each group. We used age as a covariate in all analyses. The ERSP value of each subject was extracted at each pixel location and the extracted values were correlated with the pain-related measures across subjects and across conditions for each group. Spearman Rho partial correlation coefficient and the p-value from Student's t-test were generated for each pixel location for the entire time (-1.26–7.26) and frequency range (3–90 Hz) (100 × 200 pixels in total), producing coefficient and p-value maps for each measure and for each group. Significance was set at $p < .05$ corrected for multiple comparisons using the FDR method as outlined above in Section 2.12. The analyses were conducted using MATLAB (version R2014a; MathWorks, Natick, MA).

2.14. Building VAR models

For each participant per condition, vector autoregression (VAR) modeling was conducted based on each participant's IC time series data. De-trending, determining appropriated model order, and validating the fitted model steps were conducted. Specifically, drifts in dipole-specific source time-series were first removed using a piece-wise de-trending method (Delorme et al., 2011). Then for each participant per condition, models of orders 1–25 were fitted using the Vieira-Morf lattice algorithm, and an appropriate model order was determined using information theory based criteria. We used Schwarz-Bayes criterion (Kass and Wasserman, 1995), Akaike information criterion (Bozdogan, 1987), Akaike's final prediction error criterion (Akaike, 1969), and Hannan-Quinn criterion (Hannan and Quinn, 2016), to determine four possible model orders as done in previous work (Chung et al., 2017). The mean of these four model orders was then chosen to create the final model. The model was then validated based the whiteness of the residue (i.e., autocorrelation and Portmanteau tests), the fraction of the correlation structure of the original data captured by the model (known as consistency), and its stability. The de-trending and the model order selection procedures discussed above each consisted of two important parameters: window length and moving window step size. Based on these parameters, per participant per condition, the Source Information Flow Toolbox (SIFT) estimates a VAR model per moving window and its whiteness, consistency, and stability scores are computed (Delorme et al., 2011). To obtain an optimal set of values for the window length and the moving window step size, we used a custom-built MATLAB based optimization procedure with a goal to maximize the mean (whiteness score + consistency score + stability score) computed across all participants, conditions, and moving windows. During optimization, both de-trending and the model order selection steps were constrained to share the same set of values for window length and step size. Based on the optimal window length and step size obtained from the above procedure, participant- and conditional-specific VAR modeling was conducted. In summary, the approach allowed us to derive an optimal window length and moving window step size, which were held constant across all participants and conditions. For de-trending and VAR modeling, the optimal window length was 201.5 msec. and the window step size was 121.6 msec.

2.15. Estimating effective connectivity between domain pairs

Estimating effective connectivity is based on the idea that if the past of one time series in one domain can be used to facilitate the prediction of a future time series in another domain, then one domain may have a causal influence on another domain (Granger, 1969). In this paper, we used direct directed transfer function (dDTF) to quantify the direction and the strength of information flow in the frequency domain, defined as a multiplication of DTF by partial coherence, which enables direct measures of propagation by ruling out indirect connections via mediating structures (Delorme et al., 2011; Ding et al., 2017). First, for each participant in each condition, a time-varying dDTF value for all the dipole pairs (e.g. i → j & j → i) were calculated across time points and across frequency bands (1–90 Hz). Then we extracted the weights and calculated the average value across the four frequency bands – theta: 3–8 Hz, alpha: 8–13 Hz, beta: 13–30 Hz, gamma: 70–90 Hz, and across the three time periods – baseline (-1.9 to -0.02 s), anticipation period (0.02–3.98 s) and heat stimulation period (3.98–7.82 s). Note that for the gamma frequency, we extracted the dDTF values within the higher gamma frequency range (70–90 Hz) in order to avoid line noise artifact at 60 Hz.

To estimate the information flow from a dipole in domain A to another dipole in domain B, we first computed the center of mass of the selected domain using the spatial coordinate of the contributing dipoles. For each domain, all dipoles at a distance > 6 cm from the domain center were discarded. The position of each dipole within each
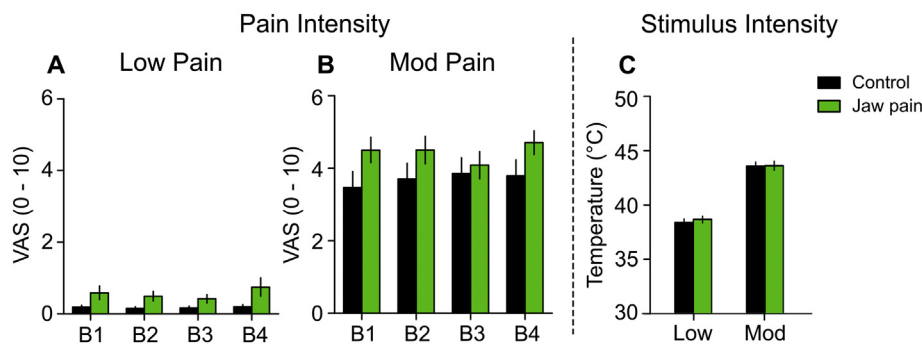
Fig. 3. Pain rating and stimulus Intensity. Mean subjective pain rating for the chronic jaw pain group (green bars) and the control group (black bars) for the low pain condition (A) and the moderate pain condition (B) across blocks. No block effect was found in either condition. In the low pain condition, the chronic jaw pain group had higher pain ratings compared to the control group ($p < .05$). In the moderate pain condition, there was no significant difference between groups ($p > .05$). Mean temperatures (i.e., stimulus intensity) for the low pain condition and the moderate pain condition for the chronic jaw pain group and the control group (C). Stimulus intensity was not significantly different between groups. VAS = Visual analog scale, B = Block, Mod = moderate.

domain was visually inspected. To compute the connectivity strength from domain A to domain B, the mean of all the dDTF values from the dipoles belonging to domain A to the dipoles belonging to domain B for the corresponding frequency band were estimated. Separate four-way ANOVAs with mixed model design with non-parametric permutation testing (Group [jaw pain, control]) X (Condition [low pain, moderate pain], Time [baseline, anticipation heat stimulation], Direction [A ➜ B, B ➜ A]) were conducted for each domain. Age was used as a covariate in all analyses. A significant interaction effect that included group was followed up with post-hoc tests. The *p*-values were FDR corrected at $p < .05$ for multiple comparisons across domains and frequencies. Data were analyzed using the R platform (Version 3.3.0) and R packages (Hadley Wickham, 2017; Wheeler and Torchiano, 2016).

2.16. dDTF and self-report questionnaire measures

To evaluate the relationship between the dDTF values and the self-report questionnaire data, partial Spearman Rho correlation tests with age as a covariate were conducted between domains at each frequency band. For the control group, partial Spearman Rho correlation tests were conducted between dDTF values and self-report measures except for the chronic pain measures (i.e. GCPS). Significance was set at $p < .05$ corrected for multiple comparisons using the FDR method.

2.17. Task-specific subjective pain rating

To assess subjective pain ratings across block, ratings within each block for each condition were first averaged. Prior to averaging, we removed trials in which a rating was not made due to recording issues or failure to make the rating. We then performed a two-way ANOVA [group (jaw pain, control) X block (4 blocks)] on the pain-intensity rating data with group as the between subjects factor and block as the within-subject factor. We performed separate ANOVAs for the low pain condition and the moderate pain condition. Degrees of freedom were adjusted when Mauchly's test of Sphericity was violated. When violated, we report the result after the Greenhouse-Giesser correction. Significance was set at $p < .05$ corrected for multiple comparisons using the Bonferroni method.

2.18. Stimulus intensity

To remain consistency with the statistical testing in the ERSP measures, separate *t*-tests were run to compare stimulus intensity between groups for the low pain and for the moderate pain condition. Block was not included in this analysis because the same temperatures were used across all blocks for each condition. Significance level was set at $p < .05$ corrected for multiple comparison using the Bonferroni method. Data were analyzed using SPSS 23.0 software (IBM Corp, Armonk, NY).

3. Results

From a total of 96 trials, an average of 94 trials per subject were analyzed for the control group and an average of 91 trials per subject were analyzed for the chronic jaw pain group.

3.1. Self-reported questionnaires

Table 1 shows that the chronic jaw pain group exhibited significant jaw functional limitations [mastication subscale: $t(17.04) = -3.17$, $p < .05$; jaw mobility subscale: $t(17.0) = -3.91$, $p < .05$; emotional and verbal expression subscale: $t(17.0) = -2.03$, $p < .05$]. The chronic jaw pain group also reported a greater number of disability days over the past 6 months [$t(17.0) = -6.98$, $p < .05$] as well as higher pain intensity [$t(17.0) = -10.9$, $p < .05$], and higher pain interference [$t(17.0) = -3.93$, $p < .05$] compared to the control group. The chronic jaw pain group reported a higher frequency of parafunctional behaviors, such as clenching teeth and pencil or pen chewing, measured by the Oral Behavior Checklist (OBC) [$t(32.0) = -4.89$, $p < .05$]. The chronic jaw pain group also reported higher levels of fatigue [$t(32.0) = -2.18$, $p < .05$]. No differences were found between groups in anxiety [$t(32.0) = -1.56$, $p > .05$] or depression [$t(32.0) = -1.45$, $p > .05$].

3.2. Subjective pain rating

Participants gave pain ratings for the low pain and for the moderate pain after each trial. Fig. 3A shows the mean task-specific ratings for each of the four blocks of experimental trials at the low pain condition and the moderate pain condition for each group. There was no block effect in the low pain condition [$F(1.8, 52.7) = 1.63$, $p > .05$] or the moderate pain condition [$F(2.6, 78.7) = 1.13$, $p > .05$], suggesting that sensitization and habituation were not significant factors in the current experiment. A significant group effect was found in the low pain condition [$F(1, 30) = 5.99$, $p < .05$], with the jaw pain group rating the stimulus 0.3 points higher than the control group. No effect of group was found in the moderate pain condition [$F(1, 30) = 2.01$, $p > .05$]. No significant interaction effect of group X block was found at the low pain condition [$F(2.6, 78.7) = 1.00$, $p > .05$] or the moderate pain condition [$F(1.8, 52.7) = 2.12$, $p > .05$].

3.3. Stimulus intensity

Fig. 3C shows the mean stimulation temperatures for the low pain condition and for the moderate pain condition for each group. For the low pain condition, the mean temperature was 38.38 °C (SD = 1.24) for the control group, and 38.64 °C (SD = 1.28) for the chronic jaw pain group. For the moderate pain condition, the mean temperature was 43.56 °C (SD = 1.44) for the control group, and 43.61 °C (SD = 1.78) for the chronic jaw pain group. No between group difference was found
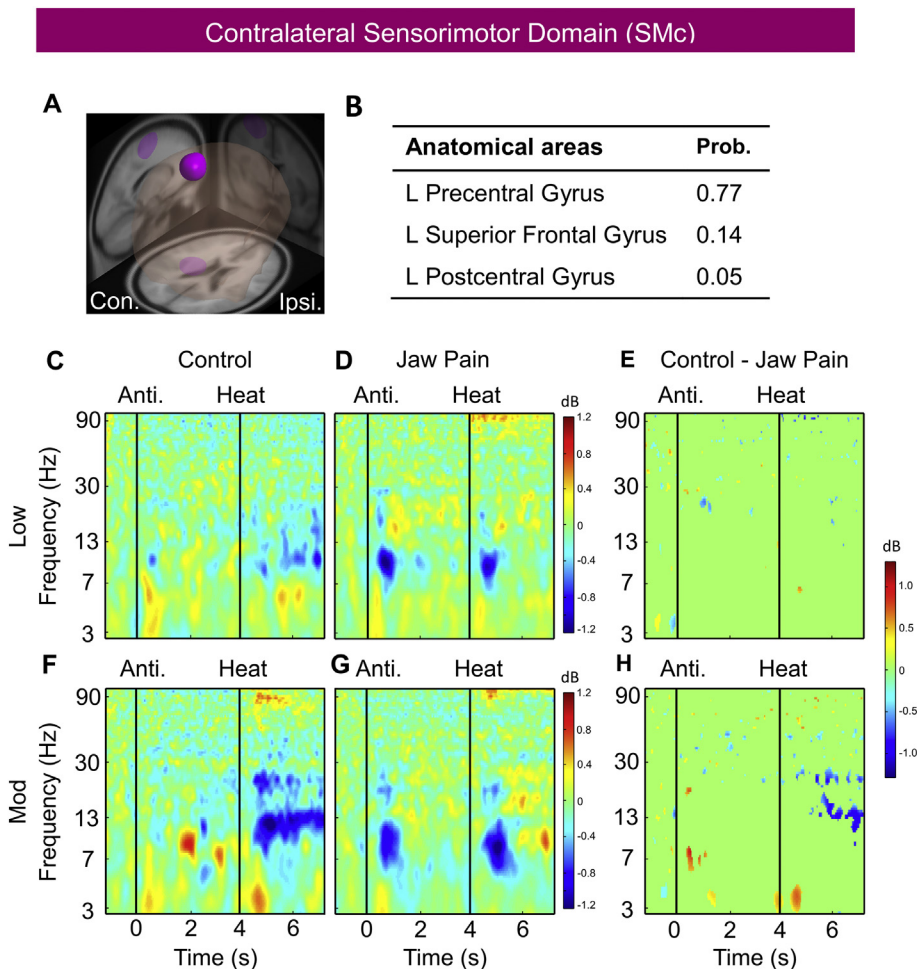
Fig. 4. Time-frequency representations from the contralateral sensorimotor domain in the chronic jaw pain group and control group. A. The sensorimotor domain revealed by the MPA analysis across participants. B. The anatomical areas identified in the domain and the fraction of the domain in each anatomical region. Anatomical localization of the domain was based on the brain atlas provided by LONI project. C. ERSP measure for the control group in the low pain condition. The two solid black lines demarcate the onset of the anticipation period (Anti. time = 0 s) and the onset of the heat stimulation (Heat. time = 4 s). Sinusoidal wavelet transform, which was used to convert the EEG data to time-frequency space, led to truncation of 740 ms from each end of the ERSP plot. The color scale represents the average increase or decrease of oscillation magnitude, relative to a pre-stimulus baseline (−2-s to 0-s before the onset of anticipation period). D. ERSP measure for the chronic jaw pain group in the low pain condition. E. The contrast plot (jaw pain – controls) in the low pain condition. F. ERSP measure for the control group in the moderate pain condition. G. ERSP measure for the chronic jaw pain group in the moderate pain condition. H. Between group contrast plot (jaw pain – controls). Mod = moderate.

for the low pain condition [$t(32.0) = −0.61$, $p > .05$], or for the moderate pain condition [$t(32.0) = −0.09$, $p > .05$], indicating no differences in the stimulus temperatures between the two groups.

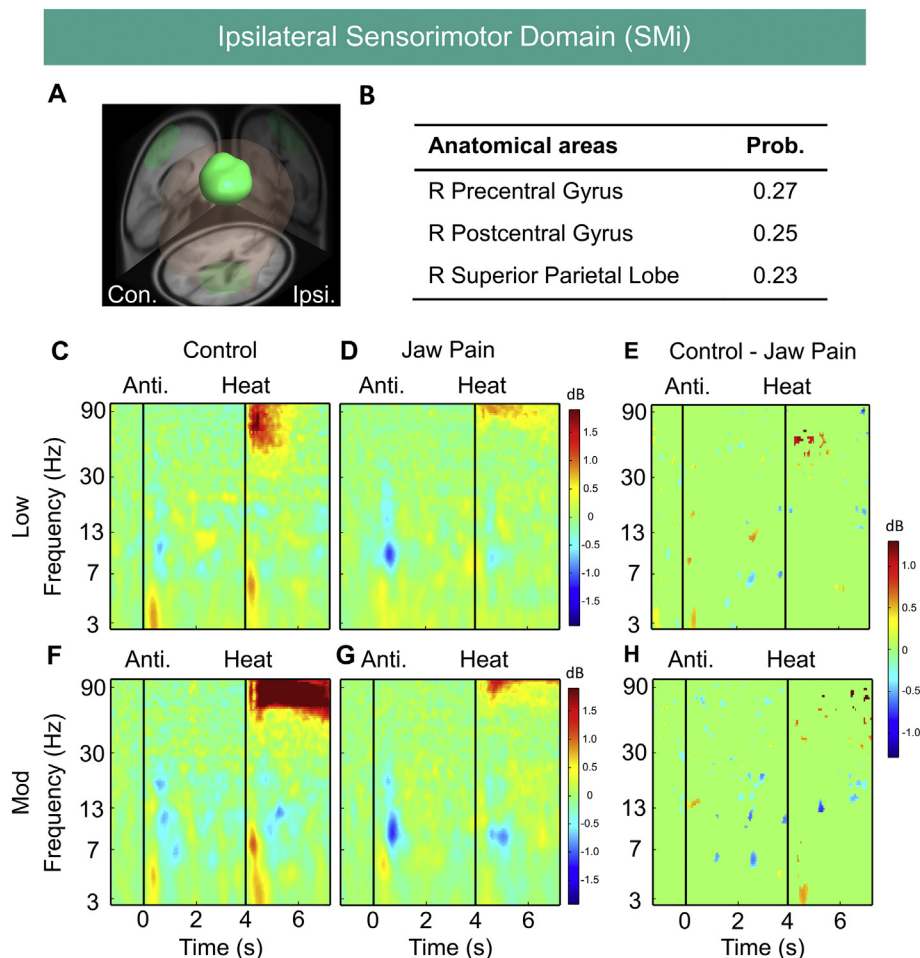### 3.4. ERSP in the contralateral sensorimotor domain (SMc)

The MPA analysis identified five domains; Two were located in the sensorimotor cortex, two in the parietal cortex, and one in the occipital cortex. Fig. 4A shows the location of the contralateral sensorimotor domain identified in the MPA analysis. The majority of the domain was positioned in the left precentral gyrus, with smaller portions of the domain positioned in the left superior frontal gyrus and left postcentral gyrus (see Fig. 4B). Fig. 4C and D show the ERSP measure from the sensorimotor domain in the control group and the jaw pain group for the low pain condition. Time is on the x-axis. The two solid black lines demarcate the onset of the anticipation period (Anti.) and the onset of the heat stimulation (Heat). Frequency is on the y-axis. The color gradients represent a change in power relative to baseline. Cool colors represent a decrease in power. Warm colors represent an increase in power. Fig. 4E shows the contrast in power between the chronic jaw pain group and the control group. No prominent differences were observed in the low pain condition. Fig. 4F shows the ERSP measure from the domain in the control group for the moderate pain condition. Increases in theta power are evident after the onset of the anticipation period and the onset of the heat stimulation period. Midway through the anticipation period, there was also an increase in alpha (red-orange dot). After the heat onset at around 4.5 s there was a reduction in power in the alpha and the beta bands that was sustained throughout the rest of the trial. Fig. 4G shows the ERSP measure in the chronic jaw pain

group for the moderate pain condition and Fig. 4H shows the contrast between groups. Although the jaw pain group show decreases in alpha and beta power after heat onset, the change in power is not sustained throughout the stimulation period. Increases in theta power immediately after each event are also attenuated relative to the control group. The contrast plots confirm these patterns and show that theta power was increased and alpha and beta power were decreased in the control group compared to the jaw pain group.

3.5. ERSP in the ipsilateral sensorimotor domain (SMi)

Fig. 5A shows the location of the ipsilateral sensorimotor domain. The majority of the domain was positioned in the right precentral and postcentral gyrus (see Fig. 5B). Fig. 5C shows the ERSP measure from the ipsilateral sensorimotor domain in the control group for the low pain condition. After onset of anticipation and heat stimulation, increases in theta power were observed. A strong increase in gamma power from 40 to 90 Hz was also evident after heat onset. Fig. 5D shows that increases in theta power were less prominent after the onset of the two events. An increase in gamma power was also evident but less prominent in the chronic jaw pain group. The contrast plot shown in Fig. 5E reveals a significant increase in theta power in the control group during the initial 1 s of the anticipation period. Fig. 5F shows a sustained and robust increase in gamma power in the control group in the moderate pain condition, which was absent in the jaw pain group (Fig. 5G). Increases in theta power after the onset of the anticipation and the heat stimulation were also absent in the jaw group. This is confirmed in the contrast plot (Fig. 5H) which shows a significant increase in theta power in the control group as compared to the jaw pain

Fig. 5. Time-frequency representations from the ipsilateral sensorimotor domain in the chronic jaw pain and control groups. A & B. The ipsilateral sensorimotor domain and the anatomical areas revealed by the MPA. C. ERSP measure for the controls in the low pain condition. D. ERSP measure for the chronic jaw pain group in the low pain condition. E. Between group contrast plot (jaw pain – controls). F. ERSP measure for the control group in the moderate pain condition. G. ERSP measure for the chronic jaw pain group in the moderate pain condition. H. Between group contrast plot (jaw pain – controls). Mod = moderate.

group after the onset of heat stimulation period.

3.6. ERSP in the contralateral parietal domain (PLc)

Within the parietal and occipital cortex, we identified three domains. The pattern of activity was similar across these domains and here we focus on the contralateral parietal domain (see Fig. 6) because the between group differences were most pronounced here. Fig. 6A shows the location of the contralateral parietal domain. The majority of the domain bridged the left superior parietal lobe, the left angular gyrus, and left superior occipital gyrus (see Fig. 6B). Fig. 6C and D show an increase in theta power immediately the onset of the anticipation period and again after the onset of the heat stimulation period in both groups. In the alpha and beta bands, brief reductions in power were followed by sustained increases in power for both groups. Fig. 6E shows the between-group contrast plot, and reveals a significant increase in theta and beta power in the jaw pain group beginning mid-way through the anticipation period and the heat stimulation period. Fig. 6F and G show ERSP data for the moderate pain condition for both groups. The patterns are similar to the low pain condition, although the modulation of power is attenuated. The contrast plot in Fig. 6H reveals an increase in power in the jaw pain group that is most evident during the heat stimulation period in the alpha and beta frequency bands. Details of the ipsilateral parietal domain and occipital domain are shown in supplementary Fig. 1 and Fig. 2.

3.7. ERSP and pain intensity in the sensorimotor domain

We conducted a separate pixel-based correlation analysis for each group for each of the three domains of interest. For the SMc domain, theta power was positively correlated with pain intensity during the heat stimulation period (4–5 s, 3–8 Hz, $p < .05$ uncorrected). No positive correlations were found between theta power in SMc and self-reported pain intensity in the jaw pain group. For the SMi domain, a negative correlation was found between theta power during the anticipation period and the subsequent pain ratings ($p < .05$ uncorrected). This pattern was absent in the jaw pain group. Although together these findings suggest a link between theta power in sensorimotor cortex and intensity ratings of an acute pain-eliciting heat stimulus in the control group, which was not evident in the jaw pain group, none of the pixels identified survived the stringent FDR correction. For the PLc domain, pain ratings in the jaw pain group negatively correlated with theta power during the anticipation period (3–4 s, 3–8 Hz, $p < .05$ uncorrected) and positively with alpha power during the heat stimulation period (6–7 s, 6–12 Hz, $p < .05$ uncorrected). However, similar to the sensorimotor domain, none of the pixels identified survived the stringent FDR correction. Correlations between pain ratings and power in the PLc domain were not found for the control group (all $p's > 0.05$).
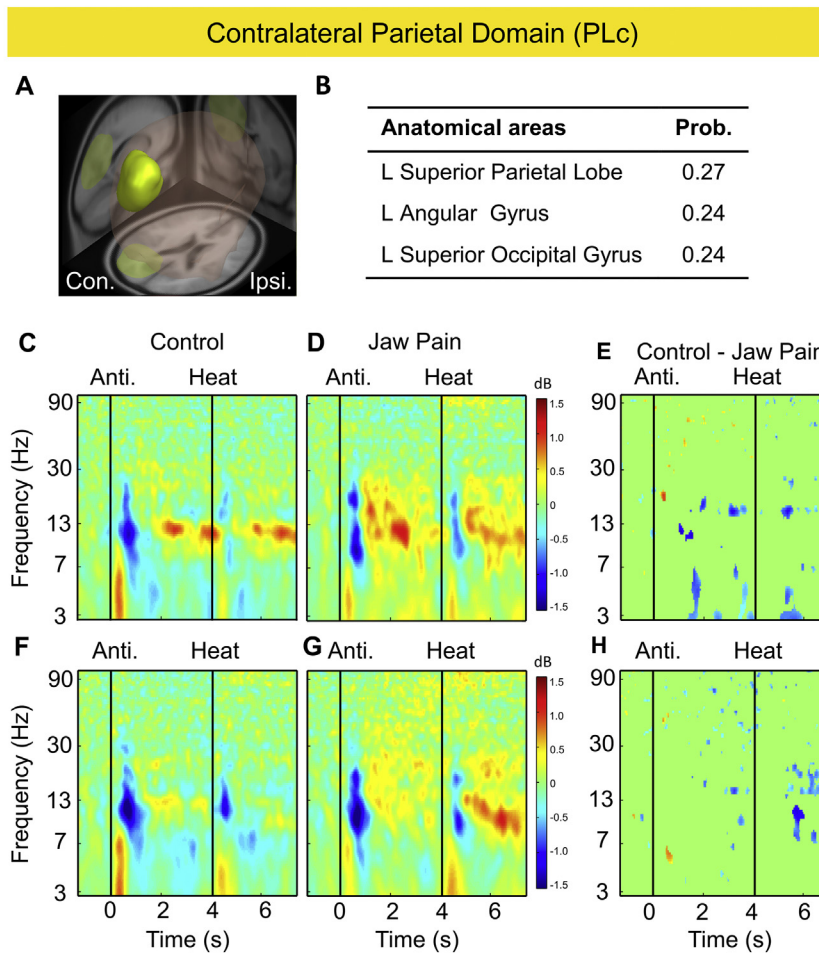
Fig. 6. Time-frequency representations from the contralateral parietal domain in the chronic jaw pain and control groups. A & B. The contralateral parietal domain and the anatomical areas revealed by the MPA. C. ERSP measure for the controls in the low pain condition. D. ERSP measure for the chronic jaw pain group in the low pain condition. E. Between group contrast plot (jaw pain – controls). F. ERSP measure for the control group in the moderate pain condition. G. ERSP measure for the chronic jaw pain group in the moderate pain condition. H. Between group contrast plot (jaw pain – controls). Mod = moderate.

3.8. Effective connectivity

We conducted separate connectivity analysis between each of the three domains of interest. *P*-values for all statistical analyses are shown in Table 1 and Table 2 in the Supplementary section. Fig. 7 shows the connectivity strength between the ipsilateral sensorimotor domain (SMi) and the contralateral parietal lobe domain (PLc) for each frequency band averaged across conditions and directions. The control group is represented by black circles and the chronic jaw pain group is represented by green circles. The three time periods (i.e. baseline,
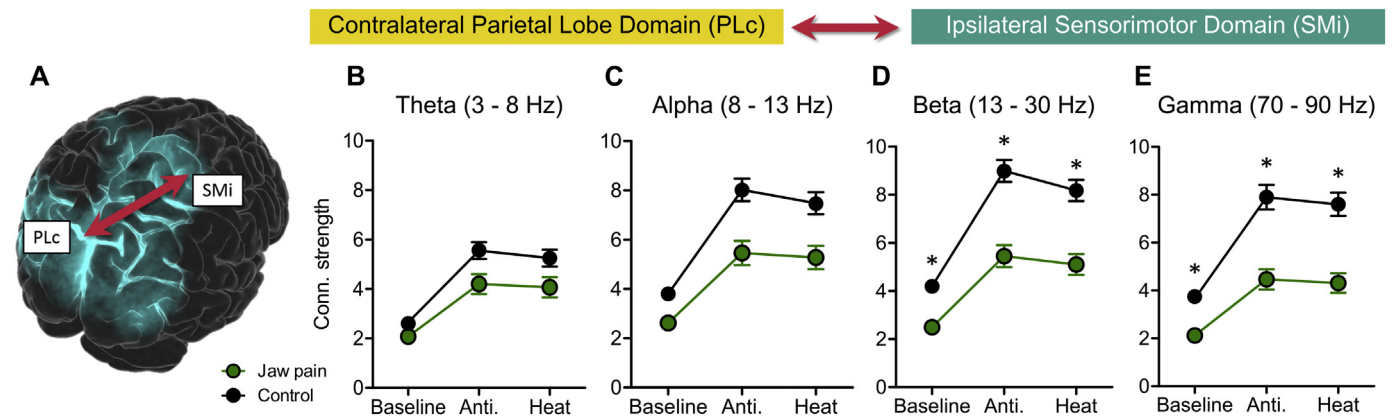
Fig. 7. Effective connectivity (dDTF). A. A significant Group x Time interaction was found between the contralateral parietal lobe domain (PLc) and the ipsilateral sensorimotor domain (SMi). Connectivity strength is shown in the theta (B), alpha (C), beta (D), and gamma (E) bands during the baseline, anticipation period, and heat stimulation period. The three time periods (i.e. baseline, anticipation, and heat stimulation) are on the x-axis. Connectivity strength is on the y-axis. Compared to the control group, the chronic jaw pain group showed significantly lower connectivity strength in the beta and gamma bands (FDR corrected at $p < .05*$) within each time period.

anticipation, and heat stimulation) are on the x-axis. Connectivity strength is on the y-axis. Fig. 7B–E show that connectivity strength was generally lower for the chronic jaw pain group. The ANOVA revealed a significant interaction between group and time in the beta band and gamma band ($p < .05$ corrected) but not in theta and alpha bands. For the beta frequency band, the between-group differences increased from 1.7 at the baseline to 3.5 during the anticipation period and to 3.1 during the heat stimulation period. For the gamma frequency band, the between-group differences increased from 1.5 at the baseline to 3.4 during the anticipation period and to 3.3 during the heat stimulation period. The Post-hoc analyses comparing groups at each time period revealed that the chronic jaw pain group had significantly lower connectivity strength during the baseline, anticipation period and the heat stimulation period across directions and conditions.

3.9. Effective connectivity and self-report questionnaire measures

Based on the significant interaction effect of group and time revealed in the ANOVA, connectivity strength between the PLc and the SMi was correlated with self-report questionnaires for each group. No significant correlation was found for either group after FDR correction.

4. Discussion

We investigated neural oscillations during the expectation and experience of an acute heat stimulus in individuals with chronic jaw pain and healthy controls. Heat stimuli were applied to the forearm, and were manipulated to evoke low pain or moderate pain. Intensity of the heat stimulus was not significantly different between groups for either condition. We report three novel findings. First, the chronic jaw pain group had a relative increase in power in alpha and beta bands and a relative decrease in power in theta and gamma bands in sensorimotor cortex. Second, the chronic jaw pain group had a relative increase in power in the alpha and beta bands in parietal cortex. Third, the chronic jaw pain group had less connectivity strength in the beta and gamma bands between sensorimotor cortex and parietal cortex. Our findings show that the effect of chronic pain attenuates rather than magnifies neural responses to heat stimuli. We interpret these findings in the context of system-level changes in intrinsic sensorimotor and attentional circuits in chronic pain.

4.1. Contralateral sensorimotor domain

Consistent with the anatomical characteristics of the spinothalamic tract, modulation of neuronal activity was most evident in the sensorimotor cortex contralateral to the effector experiencing the pain-eliciting stimulus. Our observations show that beta power was increased in the chronic jaw pain group during the pain-eliciting stimulus. Increases in beta power during resting states have been reported in chronic neurogenic pain (Sarnthein et al., 2006), fibromyalgia (González-Roldán et al., 2016), and sickle cell disease (Case et al., 2017). We extend these findings to individuals with chronic jaw pain during a task-based paradigm. Decreased beta power during a task has been interpreted as reflecting disinhibition whereas a relative increase reflects inhibition (Engel and Fries, 2010). In healthy individuals, reduced beta power in sensorimotor regions has been shown during pain-eliciting electric stimuli (Rossiter et al., 2013), laser stimuli (Hauck et al., 2015; Ploner, 2005), and heat stimuli (Misra et al., 2017b; Schulz et al., 2015). The association between beta power in sensorimotor cortex and (dis)inhibition is supported by evidence that acute pain primes the sensorimotor system such that greater reductions in beta power lead to faster reaction times (Misra et al., 2016), whereas smaller decreases or relative increases in beta power promote existing motor states (Gilbertson, 2005), slower reaction times (Kühn et al., 2004), increases in rigidity (Kühn et al., 2006), and slowed movement (Gilbertson, 2005). Converging evidence from biofeedback and

stimulation studies show that increasing beta power in the sensorimotor cortex delays movement onset (Khanna and Carmena, 2017) and slows movement down (Pogosyan et al., 2009). The relative increase in beta power in the jaw pain group in the current study may therefore reflect increased inhibition within intrinsic sensorimotor circuits. This interpretation is supported by evidence that links chronic jaw pain with changes in the speed and variability of jaw function (Hansdottir and Bakke, 2004; Wang et al., 2018) and other chronic pain conditions that are associated with slow, stiff, and less variable movement (Abboud et al., 2014; Hodges et al., 2009; Lund et al., 1991; Madeleine et al., 2008; Moseley et al., 2006; Taimela and Kujala, 1992). In short, our findings support the position that relative increases in beta power in sensorimotor cortex are a key feature of chronic pain. Moreover, they show that the disinhibition of contralateral sensorimotor cortex that is associated with acute pain in healthy controls is attenuated rather than enhanced in chronic jaw pain.

In the ipsilateral sensorimotor domain, between-group differences were less pronounced, were restricted to the gamma band, and revealed relative decreases in gamma power in the chronic jaw pain group compared to the control group. Previous studies in healthy adults have associated increases in gamma power in sensorimotor and frontal regions with increases in pain intensity (Liu et al., 2015; Misra et al., 2017a; Rossiter et al., 2013; Zhang et al., 2012). One may therefore have expected relative increases rather than decreases in the modulation of gamma power in the chronic pain group. However, our findings revealed the opposite effect with attenuated rather than enhanced gamma power responses. It is important to note however, that self-reported pain on the forearm was generally similar between groups, the between group differences in gamma power were less pronounced than in contralateral regions and were only evident in the ipsilateral sensorimotor domain. Nevertheless, the general pattern of attenuation found was consistent with responses in the alpha and beta frequencies in the contralateral domains.

4.2. Parietal domain

We report two observations in parietal cortex. First, after the onset of the anticipation and heat stimulation periods there was a brief increase in theta power and a brief decrease in alpha and beta power across both conditions. No differences were found between groups within this timeframe. This early change in power was not pain-specific, did not scale with stimulus intensity, was not altered in chronic jaw pain, and may reflect an initial orienting of attention. The link between attention and theta power over parietal cortex has been demonstrated using repeated pain-eliciting stimuli at 1 Hz (Iannetti et al., 2008). The authors demonstrated that although pain perception remained stable across pulses, theta power decreased, suggesting that the salience or novelty of the stimulus attenuated across time. Other studies show that reductions in alpha power in parietal cortex are not modality specific and can be induced by auditory, visual, sensory and pain-eliciting stimuli (Peng et al., 2012). Decreases in alpha power may reflect the release from inhibition and the engagement of cortical process (Jensen and Mazaheri, 2010; Klimesch, 2012). Our findings demonstrate that the initial orienting of attention to the heat stimulus was not influenced by chronic pain.

Following the first second after each event, between group differences did emerge in parietal cortex. The chronic jaw pain group had a relative increase in power in the alpha and beta band for both conditions. In addition to reflecting an inhibitory state, increases in alpha power also correspond with the functional suppression of irrelevant or distracting stimuli (Foxe and Snyder, 2011). Studies using lateralized visual, auditory and motor stimuli show that alpha power decreases in the contralateral hemisphere, and increases in the ipsilateral hemisphere (Haegens et al., 2010; Kerlin et al., 2010; van Dijk et al., 2010), consistent with the idea that sustained increases in attention would be more pronounced during moderate pain-eliciting compared to the low

pain-eliciting stimulation. Impaired attentional capacity has also been reported in chronic pain, which may relate to limited attentional resources, or an inability to engage attentional networks during a task (Dick et al., 2002; Dick and Rashiq, 2007; Moriarty et al., 2011). It may also be that attentional resources and threat assessment processes were consumed by ongoing pain in the jaw, resulting in fewer resources available for processing the pain-eliciting stimulus on the forearm. However, while plausible, it is difficult to square this interpretation with the finding that stimulus intensity and pain perception were generally similar between groups in the current study, and decreases in attention, or increases in distraction typically reduce pain intensity (Paris et al., 2013). Evidence from other task-based chronic pain studies suggest that the attenuated modulation of neural activity found in the current study is not unique. For instance, González-Villar et al. reported attenuated modulation of alpha power (9–12 Hz) in a cohort of fibromyalgia patients during a cognitive interference task (González-Villar et al., 2017). Sitges et al. showed attenuated power modulation across theta to beta (4–22 Hz) frequency bands over the parietal cortex in chronic musculoskeletal pain patients when viewing pleasant photos (Sitges et al., 2010). Although the stimuli from the tasks are different across these studies (i.e. viewing photos, cognitive task, heat stimulation), the common theme is that the clinical symptom of pain is not being directly evoked/exacerbated. As such, it is plausible that a general attenuation of neural activity may generalize across chronic pain conditions when completing tasks that do not evoke/exacerbate the clinical pain associated with each condition. The current findings do motivate questions on the modulation of neuronal oscillations during pain-eliciting stimuli applied to the affected body segment (e.g., jaw in the current study), where one may expect increases in attentional allocation and threat assessment, and enhanced rather than attenuated neural oscillations. Experiments that compare neural oscillations when pain-eliciting stimuli are delivered to the affected as compared to unaffected body segments would directly address this issue.

Rather than a general deficit in attention, an alternative explanation is that the chronic jaw pain group inhibited their attentional networks shortly after the onset of each cue. Although low pain and moderate pain trials were randomized, the anticipation period always correctly predicted the intensity of the heat stimulation that was delivered. In this sense, perhaps the control group remained more vigilant, or more attentive to the stimuli. Task-based fMRI studies have identified differences in brain activity in parietal cortex in chronic pain (Apkarian et al., 2001; Baliki et al., 2006; Gündel et al., 2008; Roy et al., 2018b). The BOLD signal in parietal cortex is attenuated in chronic jaw pain (Roy et al., 2018b), and decreases in the BOLD signal have been associated with increases in alpha power (Goldman et al., 2002; Ritter et al., 2009). Aurora et al. showed decreased areas of cerebral metabolism in the parietal cortex in chronic migraine using PET (Aurora et al., 2007). Together these findings suggest that relative increases in alpha power in parietal cortex may reflect a functional suppression of sustained attention.

4.3. Less connectivity strength in chronic jaw pain

The chronic jaw pain group showed less connectivity strength between sensorimotor and parietal cortex regardless of stimulus intensity. Altered connectivity patterns between brain regions have been demonstrated in chronic pain, although the neuroimaging measure and the brain regions identified vary considerably (Camfferman et al., 2017; de Tommaso et al., 2015; González-Roldán et al., 2016; Vanneste et al., 2017). Reduced activity in superior parietal and superior frontal regions was found in patients with sickle cell disease (Case et al., 2017), and fibromyalgia has been associated with decreases in lagged phase connectivity between the dorsal lateral prefrontal cortex and the posterior cingulate cortex (Vanneste et al., 2017). Chronic pain-related changes in functional connectivity have also been probed in fMRI experiments (Kucyi and Davis, 2015). Functional connectivity between

the motor cortex and the posterior insula is decreased in chronic prostatitis/chronic pelvic pain syndrome (Kutch et al., 2015), whereas increased functional connectivity during spontaneous low back pain has been found between the nucleus accumbens and prefrontal cortex (Baliki et al., 2012). Hence, communication between sensorimotor cortex and other regions decreases whereas communication between emotion and reward circuits increases (Hashmi et al., 2013). Decreased effective connectivity between sensorimotor and parietal regions may reflect a more segregated and less efficient system (Shine et al., 2016), and this system level change may alter one's ability to adapt behavior to external stimuli (Shackman et al., 2011).

Other task-based EEG studies in healthy adults have shown increases in connectivity during acute noxious stimuli (Liu et al., 2011; Ploner et al., 2009; Weiss et al., 2008), during tactile (Ploner et al., 2009), choice reaction time (Dinov et al., 2016), and movement tasks (Lu et al., 2011), and our findings converge with these to suggest that task-related increases in effective connectivity reflect the neural processes that underlie appropriate behavioral responses. A key finding in the current study is that whereas acute heat stimuli led to a general increase in effective connectivity across all participants, chronic pain had the opposite effect. When heat stimuli were experienced on an effector unrelated to the pain symptoms, effects of chronic pain and heat stimulation were not additive. Instead, they had opposite effects on connectivity strength.

5. Conclusions

Our findings provide new evidence that chronic jaw pain is associated with altered neural oscillations within and between sensorimotor cortex and parietal cortex, and suggest that these alterations reflect a relative increase in inhibition in sensorimotor and attentional networks.

Appendix A. Supplementary data

Supplementary data to this article can be found online at https://doi.org/10.1016/j.nicl.2019.101964.

References

Abboud, J., Nougarou, F., Pagé, I., Cantin, V., Massicotte, D., Descarreaux, M., 2014. Trunk motor variability in patients with non-specific chronic low back pain. European Journal of Applied Physiology 114, 2645–2654. https://doi.org/10.1007/s00421-014-2985-8.

Akaike, H., 1969. Fitting autoregressive models for prediction. Ann. Inst. Statist. Math. 21, 243–247. https://doi.org/10.1007/BF02532251.

Amari, S., 1998. Natural gradient works efficiently in learning. Neural Computation 10, 251–276. https://doi.org/10.1162/089976698300017746.

Apkarian, A.V., Thomas, P.S., Krauss, B.R., Szeverenyi, N.M., 2001. Prefrontal cortical hyperactivity in patients with sympathetically mediated chronic pain. Neuroscience Letters 311, 193–197. https://doi.org/10.1016/S0304-3940(01)02122-X.

Apkarian, A.V., Bushnell, M.C., Treede, R.-D.D., Zubieta, J.-K.K., 2005. Human brain mechanisms of pain perception and regulation in health and disease. European Journal of Pain 9, 463–484. https://doi.org/10.1016/j.ejpain.2004.11.001.

Aurora, S.K., Barrodale, P.M., Tipton, R.L., Khodavirdi, A., 2007. Brainstem dysfunction in chronic migraine as evidenced by neurophysiological and positron emission tomography studies. Headache 47, 996–1003. https://doi.org/10.1111/j.1526-4610.2007.00853.x.

Baliki, M.N., Chialvo, D.R., Geha, P.Y., Levy, R.M., Harden, R.N., Parrish, T.B., Apkarian, A.V., 2006. Chronic pain and the emotional brain: specific brain activity associated with spontaneous fluctuations of intensity of chronic Back pain. The Journal of Neuroscience 26, 12165–12173. https://doi.org/10.1523/JNEUROSCI.3576-06.2006.

Baliki, M.N., Petre, B., Torbey, S., Herrmann, K.M., Huang, L., Schnitzer, T.J., Fields, H.L., Apkarian, A.V., 2012. Corticostriatal functional connectivity predicts transition to chronic back pain. Nature Neuroscience 15, 1117–1119. https://doi.org/10.1038/nn.3153.

Benjamini, Y., Hochberg, Y., 1995. Benjamini Y, Hochberg Y. Controlling the false discovery rate: a practical and powerful approach to multiple testing. J. R. Stat. Soc. B 57, 289–300. doi:https://doi.org/10.2307/2346101.

Berger, H., 1929. Über das Elektrenkephalogramm des menschen [about the human Elektrenkephalogramm]. Arch. für Psychatrie 87, 527–570. https://doi.org/10.1055/s-0028-1130334.

Bigdely-Shamlo, N., Mullen, T., Kreutz-Delgado, K., Makeig, S., 2013. Measure projection analysis: a probabilistic approach to EEG source comparison and multi-subject inference. Neuroimage 72, 287–303. https://doi.org/10.1016/j.neuroimage.2013.01.040.

Bigdely-Shamlo, N., Mullen, T., Kothe, C., Su, K.-M., Robbins, K.A., 2015. The PREP pipeline: standardized preprocessing for large-scale EEG analysis. Frontiers in Neuroinformatics 9, 1–20. https://doi.org/10.3389/fninf.2015.00016.

Bozdogan, H., 1987. Model selection and Akaike's information criterion (AIC): the general theory and its analytical extensions. Psychometrika 52, 345–370. https://doi.org/10.1007/BF02294361.

Camfferman, D., Lorimer Moseley, G., Gertz, K., Pettet, M.W., Jensen, M.P., 2017. Waking EEG cortical markers of chronic pain and sleepiness. Pain Med. (United States) 18, 1921–1931. https://doi.org/10.1093/pm/pnw294.

Case, M., Zhang, H., Mundahl, J., Datta, Y., Nelson, S., Gupta, K., He, B., 2017. Characterization of functional brain activity and connectivity using EEG and fMRI in patients with sickle cell disease. NeuroImage Clin. 14, 1–17. https://doi.org/10.1016/j.nicl.2016.12.024.

Chung, J.W., Ofori, E., Misra, G., Hess, C.W., Vaillancourt, D.E., Burciu, R.G., Ofori, E., Stephen, A., Christou, E.A., Okun, M.S., Hess, W., Vaillancourt, D.E., 2017. Beta-band activity and connectivity in sensorimotor and parietal cortex are important for accurate motor performance. Neuroimage 144, 164–173. https://doi.org/10.1016/j.neuroimage.2016.10.008.

Coghill, R.C., Sang, C.N., Maisog, J.M., Iadarola, M.J., 1999. Pain intensity processing within the human brain: a bilateral, distributed mechanism. Journal of Neurophysiology 82, 1934–1943.

Delorme, A., Makeig, S., 2004. EEGLAB: an open source toolbox for analysis of single-trial EEG dynamics including independent component analysis. Journal of Neuroscience Methods 134, 9–21. https://doi.org/10.1016/j.jneumeth.2003.10.009.

Delorme, A., Mullen, T., Kothe, C., Akalin Acar, Z., Bigdely-Shamlo, N., Vankov, A., Makeig, S., 2011. EEGLAB, SIFT, NFT, BCILAB, and ERICA: new tools for advanced EEG processing. Computational Intelligence and Neuroscience 130714. https://doi.org/10.1155/2011/130714.

Dick, B.D., Rashiq, S., 2007. Disruption of attention and working memory traces in individuals with chronic pain. Anesthesia and Analgesia 104, 1223–1229. https://doi.org/10.1213/01.ane.0000263280.49786.f5.

Dick, B., Eccleston, C., Crombez, G., 2002. Attentional functioning in fibromyalgia, rheumatoid arthritis, and musculoskeletal pain patients. Arthritis and Rheumatism 47, 639–644. https://doi.org/10.1002/art.10800.

van Dijk, H., van der Werf, J., Mazaheri, A., Medendorp, W.P., Jensen, O., 2010. Modulations in oscillatory activity with amplitude asymmetry can produce cognitively relevant event-related responses. Proceedings of the National Academy of Sciences 107, 900–905. https://doi.org/10.1073/pnas.0908821107.

Ding, M., Truccolo, W.A., Bressler, S.L., 2017. Evaluating Causal Relations in Neural Systems: Granger Causality, Directed Transfer Function and Statistical Assessment of Significance Evaluating Causal Relations in Neural Systems: Granger Causality, Directed Transfer Function and Statistical Assess. vol. 157. pp. 145–157. https://doi.org/10.1007/s004220002235.

Dinov, M., Lorenz, R., Scott, G., Sharp, D.J., Fagerholm, E.D., Leech, R., 2016. Novel modeling of task vs. rest brain state predictability using a dynamic time warping spectrum: comparisons and contrasts with other standard measures of brain dynamics. Frontiers in Computational Neuroscience 10, 1–13. https://doi.org/10.3389/fncom.2016.00046.

Engel, A.K., Fries, P., 2010. Beta-band oscillations-signalling the status quo? Current Opinion in Neurobiology 20, 156–165. https://doi.org/10.1016/j.conb.2010.02.015.

Farella, M., Michelotti, A., Steenks, M.H., Romeo, R., Cimino, R., 2000. The diagnostic values of pressure algometry in myofascia pain of the jaw muscles. Journal of Oral Rehabilitation 27, 9–14.

Foxe, J.J., Snyder, A.C., 2011. The role of alpha-band brain oscillations as a sensory suppression mechanism during selective attention. Frontiers in Psychology 2, 1–13. https://doi.org/10.3389/fpsyg.2011.00154.

Gilbertson, T., 2005. Existing motor state is favored at the expense of new movement during 13-35 Hz oscillatory synchrony in the human corticospinal system. The Journal of Neuroscience 25, 7771–7779. https://doi.org/10.1523/JNEUROSCI.1762-05.2005.

Goldman, R.I., Stern, J.M., Engel, J., Cohen, M.S., 2002. Simultaneous EEG and fMRI of the alpha rhythm. Neuroreport 13, 2487–2492. https://doi.org/10.1097/00001756-200212200-00022.

González-Roldán, A.M., Cifre, I., Sitges, C., Montoya, P., 2016. Altered dynamic of EEG oscillations in fibromyalgia patients at rest. Pain Med. (United States) 17, 1058–1068. https://doi.org/10.1093/pm/pnw023.

González-Villar, A.J., Samartín-Veiga, N., Arias, M., Carrillo-De-La-Peña, M.T., 2017. Increased neural noise and impaired brain synchronization in fibromyalgia patients during cognitive interference. Scientific Reports 7, 1–8. https://doi.org/10.1038/s41598-017-06103-4.

Granger, C., 1969. Investigating causal relations by econometric models and cross-spectral methods. Econometrica 37, 424–438.

Gross, J., Schnitzler, A., Timmermann, L., Ploner, M., 2007. Gamma oscillations in human primary somatosensory cortex reflect pain perception. PLoS Biology 5, 1168–1173. https://doi.org/10.1371/journal.pbio.0050133.

Gündel, H., Valet, M., Sorg, C., Huber, D., Zimmer, C., Sprenger, T., Tölle, T.R., 2008. Altered cerebral response to noxious heat stimulation in patients with somatoform pain disorder. Pain 137, 413–421. https://doi.org/10.1016/j.pain.2007.10.003.

Haegens, S., Osipova, D., Oostenveld, R., Jensen, O., 2010. Somatosensory working memory performance in humans depends on both engagement and disengagement of regions in a distributed network. Human Brain Mapping 31, 26–35. https://doi.org/10.1002/hbm.20842.

Hannan, E.J., Quinn, B.G., 2016. The determination of the order of an autoregression. Journal of the Royal Statistical Society 41, 190–195.

Hansdottir, R., Bakke, M., 2004. Joint tenderness, jaw opening, chewing velocity, and bite force in patients with temporomandibular joint pain and matched healthy control subjects. Journal of Orofacial Pain 18, 108–113.

Hari, R., Baillet, S., Barnes, G., Burgess, R., Forss, N., Gross, J., Hämäläinen, M., Jensen, O., Kakigi, R., Mauguière, F., Nakasato, N., Puce, A., Romani, G.L., Schnitzler, A., Taulu, S., 2018. IFCN-endorsed practical guidelines for clinical magnetoencephalography (MEG). Clinical Neurophysiology 129, 1720–1747. https://doi.org/10.1016/j.clinph.2018.03.042.

Hashmi, J.A., Baliki, M.N., Huang, L., Baria, A.T., Torbey, S., Hermann, K.M., Schnitzer, T.J., Apkarian, A.V., 2013. Shape shifting pain: chronification of back pain shifts brain representation from nociceptive to emotional circuits. Brain 136, 2751–2768. https://doi.org/10.1093/brain/awt211.

Hauck, M., Domnick, C., Lorenz, J., Gerloff, C., Engel, A.K., 2015. Top-down and bottom-up modulation of pain-induced oscillations. Frontiers in Human Neuroscience 9, 1–8. https://doi.org/10.3389/fnhum.2015.00375.

Hodges, P., van den Hoorn, W., Dawson, A., Cholewicki, J., 2009. Changes in the mechanical properties of the trunk in low back pain may be associated with recurrence. Journal of Biomechanics 42, 61–66. https://doi.org/10.1016/j.jbiomech.2008.10.001.

Iannetti, G.D., Hughes, N.P., Lee, M.C., Mouraux, A., 2008. Determinants of laser-evoked EEG responses: pain perception or stimulus saliency? Journal of Neurophysiology 100, 815–828. https://doi.org/10.1152/jn.00097.2008.

Jensen, O., Mazaheri, A., 2010. Shaping functional architecture by oscillatory alpha activity: gating by inhibition. Frontiers in Human Neuroscience 4, 1–8. https://doi.org/10.3389/fnhum.2010.00186.

Kaneyama, K., Segami, N., Nishimura, M., Suzuki, T., Sato, J., 2002. Importance of proinflammatory cytokines in synovial fluid from 121 joints with temporomandibular disorders. The British Journal of Oral & Maxillofacial Surgery 40, 418–423. https://doi.org/10.1016/S0266-4356(02)00215-2.

Kass, R.E., Wasserman, L., 1995. A reference Bayesian test for nested hypotheses and its relationship to the schwarz criterion. Journal of the American Statistical Association. https://doi.org/10.1080/01621459.1995.10476592.

Kavanagk, R.N., Darcey, T.M., Lehmann, D., Fender, D.H., 1978. Evaluation of methods for three-dimensional localization of electrical sources in the human brain. IEEE Transactions on Biomedical Engineering BME-25, 421–429. https://doi.org/10.1109/TBME.1978.326339.

Kerlin, J.R., Shahin, A.J., Miller, L.M., 2010. Attentional gain control of ongoing cortical speech representations in a "cocktail party". The Journal of Neuroscience 30, 620–628. https://doi.org/10.1523/JNEUROSCI.3631-09.2010.

Khanna, P., Carmena, J.M., 2017. Beta band oscillations in motor cortex reflect neural population signals that delay movement onset. Elife 6, 1–31. https://doi.org/10.7554/eLife.24573.

Klimesch, W., 2012. Alpha-band oscillations, attention, and controlled access to stored information. Trends in Cognitive Sciences 16, 606–617. https://doi.org/10.1016/j.tics.2012.10.007.

Kobayashi, K., Jokaji, R., Miyazawa-Hira, M., Takatsuka, S., Tanaka, A., Ooi, K., Nakamura, H., Kawashiri, S., 2017. Elastin-derived peptides are involved in the processes of human temporomandibular disorder by inducing inflammatory responses in synovial cells. Molecular Medicine Reports 16, 3147–3154. https://doi.org/10.3892/mmr.2017.7012.

Kucyi, A., Davis, K.D., 2015. The dynamic pain connectome. Trends in Neurosciences 38, 86–95. https://doi.org/10.1016/j.tins.2014.11.006.

Kühn, A.A., Williams, D., Kupsch, A., Limousin, P., Hariz, M., Schneider, G.H., Yarrow, K., Brown, P., 2004. Event-related beta desynchronization in human subthalamic nucleus correlates with motor performance. Brain 127, 735–746. https://doi.org/10.1093/brain/awh106.

Kühn, A.A., Kupsch, A., Schneider, G.H., Brown, P., 2006. Reduction in subthalamic 8-35 Hz oscillatory activity correlates with clinical improvement in Parkinson's disease. The European Journal of Neuroscience 23, 1956–1960. https://doi.org/10.1111/j.1460-9568.2006.04717.x.

Kutch, J.J., Yani, M.S., Asavasopon, S., Kirages, D.J., Rana, M., Cosand, L., Labus, J.S., Kilpatrick, L.A., Ashe-McNalley, C., Farmer, M.A., Johnson, K.A., Ness, T.J., Deutsch, G., Harris, R.E., Apkarian, A.V., Clauw, D.J., Mackey, S.C., Mullins, C., Mayer, E.A., 2015. Altered resting state neuromotor connectivity in men with chronic prostatitis/chronic pelvic pain syndrome: a MAPP: Research Network Neuroimaging Study. NeuroImage Clin. 8, 493–502. https://doi.org/10.1016/j.nicl.2015.05.013.

Kutch, J.J., Labus, J.S., Harris, R.E., Martucci, K.T., Farmer, M.A., Fenske, S., Fling, C., Ichesco, E., Peltier, S., Petre, B., Guo, W., Hou, X., Stephens, A.J., Mullins, C., Clauw, D.J., Mackey, S.C., Apkarian, A.V., Landis, J.R., Mayer, E.A., 2017. Resting-state functional connectivity predicts longitudinal pain symptom change in urologic chronic pelvic pain syndrome: a MAPP network study. Pain 158, 1069–1082. https://doi.org/10.1097/j.pain.0000000000000886.

Lim, M, Kim, J.S., Kim, D.J., Chung, C.K., 2016. Increased low- and high-frequency oscillatory activity in the prefrontal cortex of fibromyalgia patients. Frontiers in Human Neuroscience 10, 1–11. https://doi.org/10.3389/fnhum.2016.00111.

Liu, C.C., Ohara, S., Franaszczuk, P.J., Crone, N.E., Lenz, F.A., 2011. Attention to painful cutaneous laser stimuli evokes directed functional interactions between human sensory and modulatory pain-related cortical areas. Pain 152, 2781–2791. https://doi.org/10.1016/j.pain.2011.09.002.

Liu, C.C., Chien, J.H., Chang, Y.W., Kim, J.H., Anderson, W.S., Lenz, F.A., 2015. Functional role of induced gamma oscillatory responses in processing noxious and innocuous sensory events in humans. Neuroscience 310, 389–400. https://doi.org/

10.1016/j.neuroscience.2015.09.047.

Louca Jounger, S., Christidis, N., Svensson, P., List, T., Ernberg, M., 2017. Increased levels of intramuscular cytokines in patients with jaw muscle pain. The Journal of Headache and Pain 18. https://doi.org/10.1186/s10194-017-0737-y.

Lu, C.F., Teng, S., Hung, C.I., Tseng, P.J., Lin, L.T., Lee, P.L., Wu, Y. Te, 2011. Reorganization of functional connectivity during the motor task using EEG time-frequency cross mutual information analysis. Clinical Neurophysiology 122, 1569–1579. https://doi.org/10.1016/j.clinph.2011.01.050.

Lund, J.P., Donga, R., Widmer, C.G., Stohler, C.S., 1991. The pain-adaptation model: a discussion of the relationship between chronic musculoskeletal pain and motor activity. Canadian Journal of Physiology and Pharmacology 69, 683–694. https://doi.org/10.1139/y91-102.

Madeleine, P., Mathiassen, S.E., Arendt-Nielsen, L., 2008. Changes in the degree of motor variability associated with experimental and chronic neck–shoulder pain during a standardised repetitive arm movement. Experimental Brain Research 185, 689–698. https://doi.org/10.1007/s00221-007-1199-2.

Makeig, S., Debener, S., Onton, J., Delorme, A., 2004. Mining event-related brain dynamics. Trends in Cognitive Sciences 8, 204–210. https://doi.org/10.1016/j.tics.2004.03.008.

Markiewicz, M.R., Ohrbach, R., McCall, W.D., 2006. Oral behaviors checklist: reliability of performance in targeted waking-state behaviors. Journal of Orofacial Pain 20, 306–316.

Misra, G., Coombes, S.A., 2015. Neuroimaging evidence of motor control and pain processing in the human midcingulate cortex. Cerebral Cortex 25, 1906–1919. https://doi.org/10.1093/cercor/bhu001.

Misra, G., Ofori, E., Chung, J.W., Coombes, S.A., 2016. Pain-related suppression of Beta oscillations facilitates voluntary movement. Cerebral Cortex 27, 2592–2606. https://doi.org/10.1093/cercor/bhw061.

Misra, G., Wang, W., Archer, D.B., Roy, A., Coombes, S.A., 2017a. Automated classification of pain perception using high-density electroencephalography data. Journal of Neurophysiology 117, 786–795. https://doi.org/10.1152/jn.00650.2016.

Misra, G., Wang, W., Archer, D.B., Roy, A., Coombes, S.A., Misra, G., We, W., Db, A., Roy, A., Auto-, C.S.A., 2017b. Automated classification of pain perception using high-density electroencephalography data. Journal of Neurophysiology 117, 786–795. https://doi.org/10.1152/jn.00650.2016.

Moriarty, O., McGuire, B.E., Finn, D.P., 2011. The effect of pain on cognitive function: a review of clinical and preclinical research. Progress in Neurobiology 93, 385–404. https://doi.org/10.1016/j.pneurobio.2011.01.002.

Moseley, G.L., Hodges, P.W., Lorimer Moseley, G., Hodges, P.W., Moseley, G.L., Hodges, P.W., Lorimer Moseley, G., Hodges, P.W., Moseley, G.L., Hodges, P.W., Lorimer Moseley, G., Hodges, P.W., 2006. Reduced variability of postural strategy prevents normalization of motor changes induced by back pain: a risk factor for chronic trouble? Behavioral Neuroscience 120, 474–476. https://doi.org/10.1037/0735-7044.120.2.474.

Noachtar, S., Binnie, C., Ebersole, J., Mauguiere, F., Sakamoto, A., Westmoreland, B., 1999. A glossary of terms Most commonly used by clinical Electroencephalographers and proposal for the report form for the EEG findings. In: Deuschl, G., Eisen, A. (Eds.), Recommendations for the Practice of Clinical Neurophysiology: Guidelines of the International Federation of Clinical Physiology. Elsevier Science B.V, pp. 21–40. https://doi.org/10.1055/s-2003-812583. EEG Suppl. 52.

Ofori, E., Coombes, S.A., Vaillancourt, D.E., 2015. 3D Cortical electrophysiology of ballistic upper limb movement in humans. Neuroimage 115, 30–41. https://doi.org/10.1016/j.neuroimage.2015.04.043.

Ohrbach, R., Larsson, P., List, T., 2008. The jaw functional limitation scale: development, reliability, and validity of 8- item and 20-item versions. Journal of Orofacial Pain 22, 219–230.

Paris, T.A., Misra, G., Archer, D.B., Coombes, S.A., 2013. Effects of a force production task and a working memory task on pain perception. The Journal of Pain 14, 1492–1501. https://doi.org/10.1016/j.jpain.2013.07.012.

Peng, W., Hu, L., Zhang, Z., Hu, Y., 2012. Causality in the association between P300 and alpha event-related desynchronization. PLoS One 7, e34163. https://doi.org/10.1371/journal.pone.0034163.

Peng, W., Babiloni, C., Mao, Y., Hu, Y., 2015. Subjective pain perception mediated by alpha rhythms. Biological Psychology 109, 141–150. https://doi.org/10.1016/j.biopsycho.2015.05.004.

Platt, J., Haykin, S., 1995. Information-maximization approach to blind separation and blind deconvolution. Technology 1159, 1129–1159. https://doi.org/10.1162/neco.1995.7.6.1129.

Ploner, M., 2005. Pain suppresses spontaneous brain rhythms. Cerebral Cortex 16, 537–540. https://doi.org/10.1093/cercor/bhj001.

Ploner, M., Schoffelen, J.M., Schnitzler, A., Gross, J., 2009. Functional integration within the human pain system as revealed by Granger causality. Human Brain Mapping 30, 4025–4032. https://doi.org/10.1002/hbm.20826.

Pogosyan, A., Gaynor, L.D., Eusebio, A., Brown, P., 2009. Boosting cortical activity at Beta-band frequencies slows movement in humans. Current Biology 19, 1637–1641. https://doi.org/10.1016/j.cub.2009.07.074.

Promis, S., Cella, D., Yount, S., Rothrock, N., Gershon, R., 2007. The patient-reported outcomes measurement information. Medical Care 45, 3–11.

Ritter, P., Moosmann, M., Villringer, A., 2009. Rolandic alpha and beta EEG rhythms' strengths are inversely related to fMRI-BOLD signal in primary somatosensory and motor cortex. Human Brain Mapping 30, 1168–1187. https://doi.org/10.1002/hbm.20585.

Rossiter, H.E., Worthen, S.F., Witton, C., Hall, S.D., Furlong, P.L., 2013. Gamma oscillatory amplitude encodes stimulus intensity in primary somatosensory cortex. Frontiers in Human Neuroscience 7, 1–7. https://doi.org/10.3389/fnhum.2013.00362.

Roy, A., Coombes, S.A., Chung, J.W., Archer, D.B., Okun, M.S., Hess, C.W., Shukla, A.W., Vaillancourt, D.E., 2018a. Cortical dynamics within and between parietal and motor cortex in essential tremor. Movement Disorders 34, 95–104. https://doi.org/10.1002/mds.27522.

Roy, A., Wang, W., Ho, R.L.M., Ribeiro-Dasilva, M.C., Fillingim, Roger B., Coombes, S.A., 2018b. Functional brain activity during motor control and pain processing in chronic jaw-pain. Pain 159, 2547–2564.

Sarnthein, J., Stern, J., Aufenberg, C., Rousson, V., Jeanmonod, D., 2006. Increased EEG power and slowed dominant frequency in patients with neurogenic pain. Brain 129, 55–64. https://doi.org/10.1093/brain/awh631.

Scherg, M., 1990. Fundamentals of dipole source potential analysis. In: Grandori, F., Hoke, M., Romani, G.L. (Eds.), Auditory evoked magnetic fields and electric potentials. Advances in Audiology. Karger, Basel, pp. 40–69.

Schulz, E., Tiemann, L., Schuster, T., Gross, J., Ploner, M., 2011. Neurophysiological coding of traits and states in the perception of pain. Cerebral Cortex 21, 2408–2414. https://doi.org/10.1093/cercor/bhr027.

Schulz, E., May, E.S., Postorino, M., Tiemann, L., Nickel, M.M., Witkovsky, V., Schmidt, P., Gross, J., Ploner, M., 2015. Prefrontal gamma oscillations encode tonic pain in humans. Cerebral Cortex 25, 4407–4414. https://doi.org/10.1093/cercor/bhv043.

Shackman, A.J., Salomons, T.V., Slagter, H.A., Fox, A.S., Winter, J.J., Davidson, R.J., 2011. The integration of negative affect, pain and cognitive control in the cingulate cortex. Nature Reviews. Neuroscience 12, 154–167. https://doi.org/10.1038/nrn2994.

Shattuck, D.W., Mirza, M., Adisetiyo, V., Hojatkashani, C., Salamon, G., Narr, K.L., Poldrack, R.A., Bilder, R.M., Toga, A.W., 2008. Construction of a 3D probabilistic atlas of human cortical structures. Neuroimage 39, 1064–1080. https://doi.org/10.1016/j.neuroimage.2007.09.031.

Shine, J.M., Bissett, P.G., Bell, P.T., Koyejo, O., Balsters, J.H., Gorgolewski, K.J., Moodie, C.A., Poldrack, R.A., 2016. The dynamics of functional brain networks: integrated network states during cognitive task performance. Neuron 92, 544–554. https://doi.org/10.1016/j.neuron.2016.09.018.

Sitges, C., Bornas, X., Llabrés, J., Noguera, M., Montoya, P., 2010. Linear and nonlinear analyses of EEG dynamics during non-painful somatosensory processing in chronic pain patients. International Journal of Psychophysiology 77, 176–183. https://doi.org/10.1016/j.ijpsycho.2010.05.010.

Stern, J., Jeanmonod, D., Sarnthein, J., 2006. Persistent EEG overactivation in the cortical pain matrix of neurogenic pain patients. Neuroimage 31, 721–731. https://doi.org/10.1016/j.neuroimage.2005.12.042.

Taimela, S., Kujala, U.M., 1992. Reaction times with reference to musculoskeletal complaints in adolescence. Perceptual and Motor Skills 75, 1075–1082. https://doi.org/10.2466/pms.1992.75.3f.1075.

de Tommaso, M., Trotta, G., Vecchio, E., Ricci, K., Van de Steen, F., Montemurno, A., Lorenzo, M., Marinazzo, D., Bellotti, R., Stramaglia, S., 2015. Functional connectivity of EEG signals under laser stimulation in migraine. Frontiers in Human Neuroscience 9, 1–10. https://doi.org/10.3389/fnhum.2015.00640.

Tracey, I., Mantyh, P.W., 2007. The cerebral signature for pain perception and its modulation. Neuron 55, 377–391. https://doi.org/10.1016/j.neuron.2007.07.012.

Vanneste, S., Ost, J., Van Havenbergh, T., De Ridder, D., 2017. Resting state electrical brain activity and connectivity in fibromyalgia. PLoS One 12, e0178516. https://doi.org/10.1371/journal.pone.0178516.

Von Korff, M., Ormel, J., Keefe, F.J., Dworkin, S.F., 1992. Grading the severity of chronic pain. Pain 50, 133–149. https://doi.org/10.1016/0304-3959(92)90154-4.

de Vries, M., Wilder-Smith, O.H., Jongsma, M.L.A., van den Broeke, E.N., Arns, M., van Goor, H., van Rijn, C.M., 2013. Altered resting state EEG in chronic pancreatitis patients: toward a marker for chronic pain. Journal of Pain Research 6, 815–824. https://doi.org/10.2147/JPR.S50919.

Wager, T.D., Atlas, L.Y., Lindquist, M.A., Roy, M., Woo, C.-W., Kross, E., 2013. An fMRI-based neurologic signature of physical pain. The New England Journal of Medicine 368, 1388–1397. https://doi.org/10.1056/NEJMoa1204471.

Wang, C., Rajagovindan, R., Han, S.-M., Ding, M., 2016. Top-down control of visual alpha oscillations: sources of control signals and their mechanisms of action. Frontiers in Human Neuroscience 10, 15. https://doi.org/10.3389/fnhum.2016.00015.

Wang, W., Roy, A., Misra, G., Archer, D.B., Ribeiro-Dasilva, M.C., Fillingim, R.B., Coombes, S.A., 2018. Motor-evoked pain increases force variability in chronic jaw pain. The Journal of Pain 19, 636–648. https://doi.org/10.1016/j.jpain.2018.01.013.

Weiss, T., Hesse, W., Ungureanu, M., Hecht, H., Leistritz, L., Witte, H., Miltner, W.H.R., 2008. How do brain areas communicate during the processing of noxious stimuli? An analysis of laser-evoked event-related potentials using the granger causality index. Journal of Neurophysiology 99, 2220–2231. https://doi.org/10.1152/jn.00912.2007.

Wheeler, B., Torchiano, M., 2016. lmPerm: Permutation tests for linear models. In: R Packag. Version 2.1.0.

Wickham, Hadley, 2017. Tidyverse: Easily Install and Load the "Tidyverse." R Packag. Version 1.2.1.

Winkler, I., Brandl, S., Horn, F., Waldburger, E., Allefeld, C., Tangermann, M., 2014. Robust artifactual independent component classification for BCI practitioners. Journal of Neural Engineering 11, 035013. https://doi.org/10.1088/1741-2560/11/3/035013.

Zhang, Z.G., Hu, L., Hung, Y.S., Mouraux, A., Iannetti, G.D., 2012. Gamma-band oscillations in the primary somatosensory cortex - a direct and obligatory correlate of subjective pain intensity. The Journal of Neuroscience 32, 7429–7438. https://doi.org/10.1523/JNEUROSCI.5877-11.2012.